Inorg. Chem. **2006**, *45*, 7569–7571

Ancillary Ligand Functionalization of Cyanide-Bridged $S = 6$ $Fe^{III}_4Ni^{II}_4$ Complexes for Molecule-Based Electronics

Dongfeng Li,[†] Sean Parkin,[†] Rodolphe Clérac,[‡] and Stephen M. Holmes*,[†]

Department of Chemistry, University of Kentucky, Lexington, Kentucky 40506-0055, and Centre de Recherche Paul Pascal UPR-CNRS 8641, 115 avenue du Dr. A. Schweitzer, 33600 Pessac, France

Received April 24, 2006

Treatment of 1-chloro-6-iodohexane or 1-chloro-10-iododecane with lithium tris(pyrazolyl)methanide, followed by potassium thioacetate, affords bifunctional 1-S(acetyl)-tris(pyrazolyl)alkanes (L) $(pz)_3C(CH_2)_nSAc$ ($n = 6$, **1**; 10, **2**). Magnetic studies of $\{[(pzTp)Fe^{III}(CN)_3]_4[Ni^{II}L]_4[OTf]_4\}\cdot$solvent (**4**, L = **1**; **5**, L = **2**) boxes suggest that $-(CH_2)_6$ chains (**4**) limit intermolecular interactions while $-(CH_2)_{10}$ chains in **5** introduce crystallographic disorder and a distribution of relaxation times; **4** and **5** exhibit slow relaxation of the magnetization.

The increasing demand for higher information density and circuit miniaturization is rapidly approaching the limits of device-scaling technologies, with potential cost and performance limits being realized within a decade.[1] Molecule-based electronics offer the prospect of scalable and tunable devices via judicious choice of the molecules present; systematic insertion and chemical modification of the molecules may also afford insight into the dominant conduction mechanisms that are operative.[1,2] Spin-polarized electron transport (Kondo-assisted tunneling) was recently reported in electrical devices constructed from physisorbed C_{60} between ferromagnetic nickel electrodes.[1e] Tunneling magnetoresistance (TMR) through the fullerenes (≤40% at 1.5 K) was also found, suggesting that simple resistance measurements can probe the quantum state of electrically isolated molecules;[1e] the modest TMR value is likely due to the low spin state and inefficient electronic coupling of the fullerenes to the electrodes.

We reasoned that covalently linked paramagnetic (or magnetic) complexes ($S > {}^1/_2$) bridging magnetic electrodes (e.g., Co, Ni, Fe/Ni) would afford more efficient molecule-based spin valves under ideal conditions.[1,2] Via modified synthetic strategies developed for self-assembled monolayers and single-molecule magnets appended to gold surfaces, we prepared a series of polynuclear magnetic complexes containing poly(pyrazol-1-yl)borate tricyanoferrate(III)[3] and easily modified ancillary ligands (Figure 1)[1,2,4−6] for use in molecule-based devices; integration of $\{Fe^{III}_4[Ni^{II}L]_4\}$ cubes into nanoscale tunnel junctions afford apparent molecule-based devices that function at 300 K.[2c]

Furthermore, systematic modification of the ancillary ligands may also assist our understanding of the spin transport mechanisms operative in these molecule-based devices, the origin of unusual magnetization relaxation behavior in $\{Fe^{III}_4[Ni^{II}\{(pz)_3C_2H_2OH\}]_4\}^{4+}$ cubes, and allow

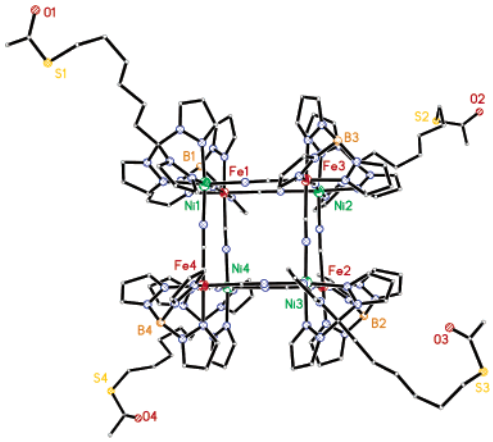

Figure 1. X-ray structure of **4**. All anions, H atoms, pendant pyrazoles, and disordered S(acetyl)-hexyl chains were removed for clarity. Selected bond distances (Å) and angles (deg): Fe1−C11, 1.950(6); Ni1−N11, 2.078(5); Fe1···Ni1, 5.188(5); Fe2···Fe4, 7.434(6); Ni1···Ni3, 7.175(6); C11−Fe1−C12, 88.2(2); N11−Ni1−N21, 92.6(2).

* To whom correspondence should be addressed. E-mail: smholm2@uky.edu.

[†] University of Kentucky.

[‡] Centre de Recherche Paul Pascal, UPR-CNRS 8641.

(1) (a) Metzger, R. M. *Chem. Rev.* **2003**, *103*, 3803−3834. (b) Tour, J. M.; Jones, L., II; Pearson, D. L.; Lamba, J. J. S.; Burgin, T. P.; Whitesides, G. M.; Allara, D. L.; Parikh, A. N.; Atre, S. V. *J. Am. Chem. Soc.* **1995**, *117*, 9529−9534. (c) Park, J.; Pasupathy, A. N.; Goldsmith, J. I.; Chang, C.; Yaish, Y.; Petta, J. R.; Rinkoski, M.; Sethna, J. P.; Abruña, H. D.; McEuen, P. L.; Ralph, D. C. *Nature* **2002**, *417*, 722−725. (d) Liang, W.; Shores, M. P.; Bockrath, M.; Long, J. R. *Nature* **2002**, *417*, 725−729. (e) Pasupathy, A. N.; Bialczak, R. C.; Martinek, J.; Grose, J. E.; Donev, L. A. K.; McEuen, P. L.; Ralph, D. C. *Science* **2004**, *306*, 86−89. (f) Prinz, G. A. *Science* **1998**, *282*, 1660−1663. (g) Prinz, G. A. *Science* **1999**, *283*, 330−333.

(2) (a) Cornia, A.; Fabretti, A. C.; Pacchioni, M.; Zobbi, L.; Bonacchi, D.; Caneschi, A.; Gatteschi, D.; Biagi, R.; Del Pennino, U.; De Renzi, V.; Gurevich, L.; Van der Zant, H. S. J. *Angew. Chem., Int. Ed.* **2003**, *42*, 1645−164. (b) Gryko, D. T.; Clausen, C.; Lindsey, J. S. *J. Org. Chem.* **1999**, *64*, 8635−8647. (c) Tyagi, P.; Li, D.; Holmes, S. M.; Hinds, B. J., submitted for publication. (d) Mannini, M.; Bonacchi, D.; Zobbi, L.; Piras, F. M.; Speets, E. A.; Caneschi, A.; Cornia, A.; Magnani, A.; Ravoo, B. J.; Reinhoudt, D. N.; Sessoli, R.; Gatteschi, D. *Nano Lett.* **2005**, *5*, 1435−1438. (e) Coronado, E.; Forment-Aliga, A.; Romero, F. M.; Corradini, V.; Biagi, R.; De Renzi, V.; Gambardella, A.; Del Pennino, U. *Inorg. Chem.* **2005**, *44*, 7693−7695.

10.1021/ic060695q CCC: $33.50
Published on Web 08/18/2006

Scheme 1. General Synthesis of Tripodal S(acetyl)-tris(pyrazolyl)alkanes

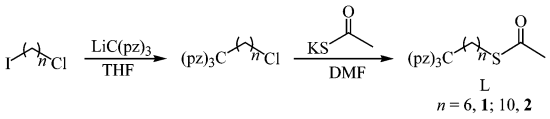

for tuning of cluster anisotropy barriers.[2c,3a,4] In the present Communication, we report the synthetic, spectroscopic, structural, and magnetic details of several structurally related $\{Fe^{III}_4Ni^{II}_4\}$ complexes.

The synthesis of two 1-S(acetyl)-tris(pyrazolyl)alkanes is illustrated in Scheme 1. Treatment of tris(pyrazolyl)methane with stoichiometric quantities of *n*-butyllithium in tetrahydrofuran (THF), followed by dropwise addition of 1-chloro-6-iodohexane or 1-chloro-10-iododecane and potassium thioacetate, readily affords 1-S(acetyl)-functionalized tris(pyrazolyl)alkanes, $[(pz)_3C(CH_2)_nSAc$; $n = 6$, **1**; 10, **2**] as yellow oils.[3i] The IR spectra of **1** and **2** exhibit intense pyrazole ($\nu_{C=N}$) and thioacetyl ($\nu_{C=O}$ and ν_{S-CO}) stretching absorptions at ca. 1515, 1690, and 628 cm^{-1}, respectively.[3i] The ^1H NMR spectrum of **1** exhibits several multiplets due to alkyl methylenes at 1.38 (4H), 1.54 (4H), and 3.28 (2H) ppm, in addition to a singlet [δ 2.32, $CH_3C(O)$, 3H] and a triplet [δ 2.83, CH_2S, 2H] that are assigned as acetyl methyl and methylene groups adjacent to the S atom. Additional resonances, tentatively assigned as inequivalent pyrazole protons, are also found at 6.31, 7.01, and 7.68 ppm in a 1:1:1 ratio. For **2**, the alkyl resonances are found between 1.19 and 1.61 ppm in addition to a downfield multiplet at 3.29 ppm and triplet (3.26 ppm, CH_2S), singlet (2.33 ppm, CH_3), and pyrazole resonances that are similar to those in **1**.[3i,5]

Treatment of $[NEt_4][(pzTp)Fe^{III}(CN)_3]$[3a] [pzTp = tetra(pyrazol-1-yl)borate][5a] with nickel(II) trifluoromethanesulfonate in dimethylformamide (DMF), followed by 2,2,2-tris(pyrazol-1-yl)ethanol (L^1),[5b] affords dark-red crystals of $\{[(pzTp)Fe^{III}(CN)_3]_4[Ni^{II}L^1]_4[OTf]_4\}\cdot 10DMF\cdot Et_2O$ (**3**).[3a] In an analogous manner, substitution of L for **1** and **2** affords additional $\{[(pzTp)Fe^{III}(CN)_3]_4[Ni^{II}L]_4[OTf]_4\}$ (**4**, L = **1**; **5**, L = **2**) boxes. IR spectra of **3**−**5** exhibit an intense ν_{CN} stretching absorption at 2174 cm^{-1}, which is shifted to higher energy relative to $[NEt_4][(pzTp)Fe^{III}(CN)_3]$ (2120 cm^{-1}), indicating that bridging cyanides are present;[3,5c,6a] additional absorptions at 1672 and 1684 cm^{-1} signal the presence of intact S(acetyl) groups in **4** and **5**.[2]

Compounds **3** and **4** crystallize in tetragonal ($I4_1/acd$) and monoclinic ($P2_1/c$) space groups, respectively.[3a,i] To date, only microcrystalline powders of **5** have been available, precluding single-crystal diffraction studies. In **3** and **4**, the Fe^{III} and Ni^{II} centers reside in alternate corners of a slightly distorted box and are linked via cyanides (Figure 1). For **4**, the bridging cyanide Fe−C and Ni−N bond distances range from 1.939(6) to 1.957(6) Å and from 2.050(6) to 2.082(5) Å, while the average C−Fe−C and N−Ni−N bond angles are 87.9(3) and 92.9(2)°; the corresponding average edge (Fe1···Ni2), face (Fe1···Fe2), and body-diagonal (Fe1···Ni3) distances are ca. 5.120(3), 7.364(4), and 8.858(4) Å, respectively. The closest intermolecular contacts [3.513(4) Å] are found between the alkyl chains and the pyrazole C atoms in **4**; for **3**, the closest contact between pendant pyrazoles is 3.668(4) Å.[3i]

For **4** and **5**, the $\chi_M T$ vs T data suggest that the Fe^{III} and Ni^{II} centers are ferromagnetically coupled (Figures 2, S2, and S3 in the Supporting Information) because $\chi_M T$ gradually increases from 7.9 and 7.5 $cm^3\ K\ mol^{-1}$ (300 K) to maximum values of 22.8 and 22.9 $cm^3\ K\ mol^{-1}$ at 5.0 K, respectively.[3,5,6a] Assuming that **3**−**5** are structurally related, the magnetic data were simulated (MAGPACK)[7a] via the following Hamiltonian: $H = -2J_{iso}[S_1(S_6 + S_7 + S_8) + S_2(S_5 + S_7 + S_8) + S_3(S_5 + S_6 + S_8) + S_4(S_5 + S_6 + S_7)]$, where J_{iso} is the isotropic exchange between the low-spin Fe^{III} and Ni^{II} sites and S_i is the spin operator for each metal center ($S_i = 1$, Ni^{II}, $i = 1-4$; $S_i = {}^1/_2$, Fe^{III}, $i = 5-8$). Neglecting the magnetic data below 30 K, to avoid possible effects of the magnetic ground-state anisotropy and intercluster interactions, the calculated values of g_{iso} are 2.3, 2.3, and 2.3 while the J_{iso} values are 9.5(5), 9.5(5), and 8.5(5) K for **3**−**5**, respectively.[3i] As expected for low-spin Fe^{III} ($S = {}^1/_2$) centers that exhibit orbital contribution to the magnetic moment, the g_{iso} value deviates significantly from 2.[3,6a] The magnitudes of the magnetic exchange interactions are also comparable to a variety of polynuclear complexes containing Fe^{III} and Ni^{II} centers.[3,6a]

Considering the estimated values of J_{iso}, the first excited states ($S = 5$) for **3**−**5** are ca. 23.2, 23.2, and 20.7 K above

(3) (a) Li, D.; Parkin, S.; Wang, G.; Yee, G. T.; Clérac, R.; Wernsdorfer, W.; Holmes, S. M. *J. Am. Chem. Soc.* **2006**, *128*, 4214−4215. (b) Li, D.; Parkin, S.; Wang, G.; Yee, G. T.; Prosvirin, A. V.; Holmes, S. M. *Inorg. Chem.* **2005**, *44*, 4903−4905. (c) Wang, S.; Zou, J.-L.; Zhou, H.-C.; Choi, H. J.; Ke, Y.; Long, J. R.; You, X.-Z. *Angew. Chem., Int. Ed.* **2004**, *43*, 5940−5943. (d) Kim, J.; Han, S.; Cho, I.-K.; Choi, K. Y.; Heu, M.; Yoon, S.; Suh, B. J. *Polyhedron* **2004**, *23*, 1333−1339. (e) Wang, S.; Zuo, J.-L.; Zhou, H.-C.; Song, Y.; You, X.-Z. *Inorg. Chim. Acta* **2005**, *358*, 2101−2106. (f) Wang, S.; Zuo, J.-L.; Zhou, H.-C.; Song, Y.; Gao, S.; You, X.-Z. *Eur. J. Inorg. Chem.* **2004**, 3681−3687. (g) Lescouëzec, R.; Vaissermann, J.; Lloret, F.; Julve, M.; Verdaguer, M. *Inorg. Chem.* **2002**, *41*, 5943−5945. (h) Kim, J.; Han, S.; Cho, I.-K.; Choi, K. Y.; Heu, M.; Yoon, S.; Suh, B. J. *Polyhedron* **2004**, *23*, 1333−1339. (i) See the Supporting Information.

(4) Accorsi, S.; Barra, A.-L.; Caneschi, A.; Chastanet, G.; Cornia, A.; Fabretti, A. C.; Gatteschi, D.; Mortalò, C.; Olivieri, E.; Parenti, F.; Rosa, P.; Sessoli, R.; Sorace, L.; Wernsdorfer, W.; Zobbi, L. *J. Am. Chem. Soc.* **2006**, *128*, 4742−4755.

(5) (a) Trofimenko, S. *Scorpionates, The Coordination Chemistry of Polypyrazolylborate Ligands*; Imperial College Press: London, 1999. (b) Reger, D. L.; Grattan, T. C.; Brown, K. J.; Little, C. A.; Lamba, J. J.; Rheingold, A. L.; Sommer, R. D. *J. Organomet. Chem.* **2000**, *607*, 120−128. (c) Nakamoto, K. *Infrared and Raman Spectra of Inorganic and Coordination Compounds*, 5th ed; Wiley: New York, 1997.

(6) (a) Yang, J. Y.; Shores, M. P.; Sokol, J. J.; Long, J. R. *Inorg. Chem.* **2003**, *42*, 1403−1419. (b) Schelter, E. J.; Prosvirin, A. V.; Dunbar, K. R. *J. Am. Chem. Soc.* **2004**, *126*, 15004−15005. (c) Berlinguette, C. P.; Vaughn, D.; Cañada-Vilalta, C.; Galán-Mascarós, J. R.; Dunbar, K. R. *Angew. Chem., Int. Ed.* **2003**, *42*, 1523−1526. (d) Sokol, J. J.; Hee, A. G.; Long, J. R. *J. Am. Chem. Soc.* **2002**, *124*, 7656−7657. (e) Sessoli, R.; Gatteschi, D. *Angew. Chem., Int. Ed.* **2003**, *42*, 268−297. (f) Beltran, L. M. C.; Long, J. R. *Acc. Chem. Res.* **2005**, *38*, 325−334.

(7) (a) Borras-Almenar, J. J.; Clemente-Juan, J. M.; Coronado, E.; Tsukerblat, B. S. *J. Comput. Chem.* **2001**, *22*, 985−991. (b) Boskovic, C.; Bircher, R.; Tregenna-Piggott, P. L. W.; Güdel, H.; Paulsen, C.; Wernsdorfer, W.; Barra, A. L.; Khatsko, E.; Neels, A.; Stoeckli-Evans, H. *J. Am. Chem. Soc.* **2003**, *125*, 14046−14058. (c) Miyasaka, H.; Nakata, K.; Lecren, L.; Coulon, C.; Nakazawa, Y.; Fujisaki, T.; Sugiura, K.-I.; Yamashita, M.; Clérac, R. *J. Am. Chem. Soc.* **2006**, *128*, 3770−3783. (d) Chakov, N. E.; Wernsdorfer, W.; Abboud, K. A.; Christou, G. *Inorg. Chem.* **2004**, *43*, 5919−5930.

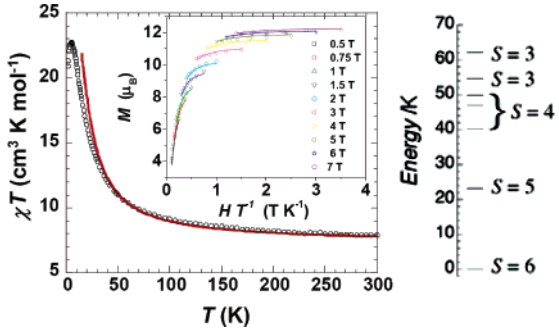

Figure 2. χT vs T plot for **4** at $H = 0.1$ T (left). Red line: MAGPACK simulation of the data above 30 K. Inset: Plot of reduced magnetization vs H/T between 2 and 5 K. Solid lines represent least-squares fittings of the data. Energy level diagram for **4** (right).

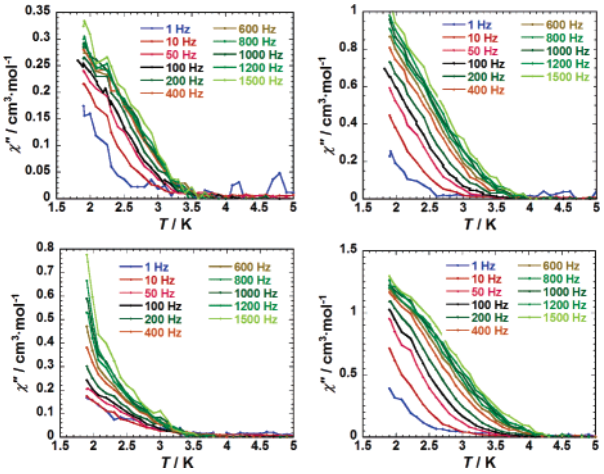

Figure 3. Top: Temperature dependence of the imaginary (χ'') components of the ac susceptibility for **4** (left) and **5** (right) ($H_{dc} = 0$ G and $H_{ac} = 3.5$ G) between 1 and 1500 Hz. Bottom: χ'' vs T data for **4** (left) and **5** (right) at $H_{dc} = 800$ and 1000 G, respectively ($H_{ac} = 3.5$ G).

the $S = 6$ ground state. Confirmation of the $S = 6$ ground state is found in the field dependence of the magnetization measurements at 1.85 K because M approaches 12 μ_B at 7 T (Figures S4 and S5 in the Supporting Information) for **3**−**5**. Least-squares fitting of the M vs H/T data (ANISOFIT) affords $D/k_B = -0.33$, -0.35, and -0.33 K, suggesting that the maximum energy barriers for **3**−**5** are $\Delta = |D|S_T^2/k_B = 11.9$, 12.6, and 11.9 K (Figures 2, inset, and S7 in the Supporting Information).[3a,i]

To further probe suspected slow magnetization relaxation behavior, the temperature dependence of the ac susceptibility was measured at various frequencies at $H_{dc} = 0$ Oe (Figures 3, S8, and S9 in the Supporting Information). Compound **3** exhibits rather small frequency-independent χ'' values that are ca. 100 times smaller than χ', while **4** and **5** exhibit χ'' values that are ca. 35 and 13 times smaller than χ', respectively (Figures 3, S8, and S9 in the Supporting Information).[3a,i] Initially, the small χ'' signals were attributed to an undefined magnetic species, but the frequency dependence of χ'' at 1.8 K in the presence of nonzero H fields suggests that **3** exhibits slow relaxation of the magnetization, with two intrinsic characteristic times in the 1−1500-Hz frequency range at 1.85 K.[3a] The origin of the two relaxation modes in **3** remains unclear, but qualitatively similar behavior has been reported by Boskovic et al. for $[Mn_4Cl_4(L')_4]$[7b] (H_2L' = 4-*tert*-butylsalicylidene-2-ethanolamine) and Miyasaka et al. for $[Mn_4(hmp)_4Br_2(OMe)_2(dcn)_2]\cdot 0.5H_2O\cdot 2THF$[7c] [Hhmp = 2-(hydroxymethyl)pyridine]. In both cases, this feature has been attributed to intercomplex interactions, but crystallographic disorder or phonon-bottleneck effects may also be important.[7d] In **4**, a single relaxation mode has been observed during the course of our studies (Figure S10 in the Supporting Information). This high-frequency relaxation behavior is comparable to that observed for **3** at zero and nonzero applied dc fields (Figures 3 and S10 in the Supporting Information),[3a] suggesting that the low-frequency relaxation behavior is linked, as suspected, to the presence of intermolecular interactions. These interactions are presumably suppressed by the $-(pz)_3C(CH_2)_6SAc$ chains present in **4**, while even longer chains [$-(pz)_3C(CH_2)_{10}SAc$, **5**] afford similar behavior (Figure 3). Nevertheless, the frequency dependence of the ac susceptibility (Figure S11 in the Supporting Information) suggests that these $\{Fe^{III}_4Ni^{II}_4\}$ complexes exhibit a distribution of relaxation times and, concomitantly, a broad relaxation mode is observed. This result seems to be correlated with our inability to isolate single crystals of **5**, which is probably a consequence of extensive crystallographic disorder induced by the long alkyl chains. It is worth noting that this unusual relaxation remains field-dependent, as is often observed for single-molecule magnets that exhibit fast quantum tunneling of the magnetization in zero dc field (Figure S11 in the Supporting Information).

In summary, we have described the syntheses, structures, and magnetic properties of two new cyanometalate $S = 6$ anisotropic complexes that exhibit slow relaxation of magnetization. In **4**, the hexyl chains limit intermolecular interactions between the $\{Fe^{III}_4[Ni^{II}L]_4\}$ complexes, while the longer decyl chains in **5** induce crystallographic disorder, which leads to a distribution of relaxation times, as suggested by the ac susceptibility measurements.

Acknowledgment. S.M.H. gratefully acknowledges the donors of the American Chemical Society Petroleum Research Fund (PRF 38388-G3), the Kentucky Science and Engineering Foundation (Grants KSEF-621-RDE-006 and KSEF-992-RDE-008), and the University of Kentucky Summer Faculty Research Fellow and Major Research Project programs for financial support. R.C. thanks MAGMANet (NMP3-CT-2005-515767), the CNRS, the University of Bordeaux 1, and the Conseil Régional d'Aquitaine for financial support. The authors are also grateful to E. Coronado and J. R. Long for providing the MAGPACK and ANISOFIT programs.

Supporting Information Available: X-ray crystallographic data (CIF format, **4**) and synthetic details and additional magnetic data (Figures S1−S11). This material is available free of charge via the Internet at http://pubs.acs.org.

IC060695Q